PCCP

COMMUNICATION

Build-up of symmetry breaking using a titanium suboxide in bulk-heterojunction solar cells†

Jung Hwa Seo,[a] **Heejoo Kim**[b] **and Shinuk Cho*[c]**

The importance of symmetry breaking was investigated in bulk heterojunction solar cells with a conventional device structure. Artificial symmetry breaking was built up by introducing a titanium suboxide. With sufficient symmetry breaking, the influence of the cathode work-function can be diminished, thereby extracting the same level of open circuit voltage regardless of metal work-function.

Polymer bulk heterojunction (BHJ) solar cells based on composites of semiconducting conjugated polymers and fullerene derivatives have received much attention because of their potential application in low-cost, printable, portable, and flexible renewable energy sources.[1–3] Tremendous effort has been devoted to the development of materials and morphological structures that facilitate enhanced device performance. Recently, encouraging progress has been made with regard to enhancements in the power conversion efficiency (PCE) of BHJ solar cells, with over 8% PCE values having been reported.[4–7]

The operating principle of BHJ solar cells is based on photo-induced charge transfer and separation between semiconducting polymers and soluble fullerenes.[8] After charge separation, created holes and electrons must move to the anode and cathode so as to generate photocurrents. However, a BHJ mixture has no prior symmetry breaking in its volume due to the different frontier molecular energy levels and work functions (WFs) of the electrodes. Therefore, in order to induce an efficient drift of charge carriers, a symmetry breaking condition is essential in BHJ solar cells.

In conventional single solar cells, symmetry breaking is simply created by the different WFs of the electrodes. Indium tin oxide (ITO, WF = 4.7 eV) is normally used as an anode (transparent electrode) in such devices. Therefore, the use of a metal with a WF lower than that of ITO can induce sufficient symmetry breaking. However, the selection of a suitable metal for the cathode is not simple. Low WF metals such as Ca and Mg are

[a] Department of Materials Physics, Dong-A University, Busan 604-714, Republic of Korea
[b] Heeger Center for Advanced Materials & Research Institute for Solar and Sustainable Energies, Gwangju 500-712, Republic of Korea
[c] Department of Physics and EHSRC, University of Ulsan, Ulsan 680-749, Republic of Korea. E-mail: sucho@ulsan.ac.kr; Fax: +82-52-259-1693; Tel: +82-52-259-1268

not stable in air, which limits the lifetime of devices. On the other hand, the use of air-stable noble metals such as Ag (WF = 4.7 eV) and Au (WF = 5.1 eV) leads to poor device performance because their high WF induces reverse symmetry breaking.

Up to now, symmetry breaking has been emphasized only in inverted solar cells. In inverted solar cells, it is often preferable to use Ag as an anode metal. However, because Ag has a WF similar to that of ITO, symmetry breaking is not spontaneously created. Thus, an additional functional layer that induces symmetry breaking must be used in inverted solar cells.[9–11] Since symmetry breaking was thought to be created spontaneously in conventional solar cells through the use of different WF metals, the role of symmetry breaking is not often considered.

In this communication, we describe our investigation of the importance of symmetry breaking in BHJ solar cells with a conventional device structure. Titanium suboxide (TiO$_x$) was used as the material that induces symmetry breaking. Since TiO$_x$ exhibits selective charge transfer properties (hole blocking and electron transferring),[4,12,13] artificial symmetry breaking is built up during charge transport. In addition, various cathode metals (Al, Ag, and Au) were used to explore the effects of the TiO$_x$ symmetry breaking layer.

Shown in Fig. 1a is a schematic diagram of the device structure together with the chemical structures of the active materials, poly[*N*-9″-hepta-decanyl-2,7-carbazole-*alt*-5,5-(4′,7′-di-2-thienyl-2′,1′,3′-benzothiadiazole)] (PCDTBT) and [6,6]-phenyl-C$_{71}$-butyric methyl ester (PC$_{71}$BM). The TiO$_x$ layer was prepared using sol–gel chemistry as described in detail elsewhere.[12] Energy level diagrams of each component are displayed in Fig. 1b.

Shown in Fig. 2 are the current density–voltage (*J–V*) characteristics obtained under illumination for PCDTBT:PC$_{71}$BM solar cells that were fabricated using either Al, Ag, or Au as the cathode with and without a TiO$_x$ symmetry breaking layer. For the solar cells without the TiO$_x$ layer, all parameters were significantly influenced by the WF of the cathodes, as shown in Fig. 2a. A variation of ∼0.5 mA cm^{-2} in the short-circuit current (J_{sc}) was confirmed *via* external quantum efficiency (EQE) measurements obtained for each device (ESI†, Fig. S1). The fill factor (FF) of the Ag device (45%) was smaller than that of the Al device (50%), while the Au device exhibited the largest decrease in the J_{sc} and FF.

The difference in the open-circuit voltage (V_{oc}) was particularly noticeable for the various cathodes; the V_{oc} of the devices with Al, Ag, and Au cathodes were 0.82, 0.66, and 0.55 V, respectively.
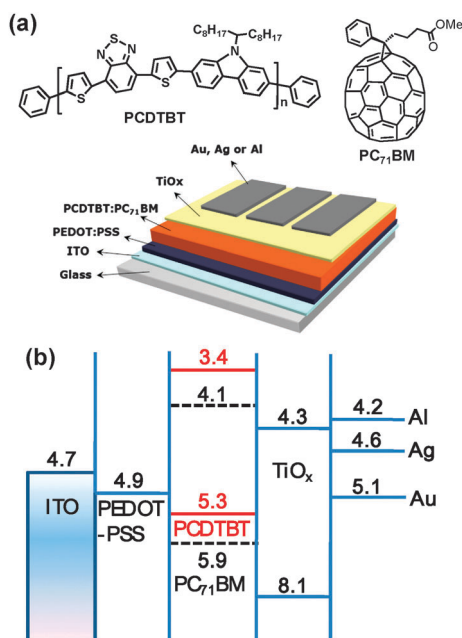
Fig. 1 (a) Schematic diagram of the device structure and the chemical structures of PCDTBT and $PC_{71}BM$. (b) Energy level diagrams of the BHJ components.
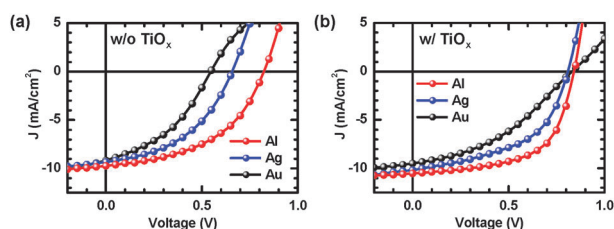

Fig. 2 J–V characteristics of the $PCDTBT:PC_{71}BM$ solar cells on various cathodes (a) without and (b) with a TiO_x interlayer under illumination with an AM 1.5G solar simulator (100 mW cm^{-2}).

The device with an Al cathode (without the TiO_x layer) exhibited a higher V_{oc} than the Ag and Au devices, indicating the existence of a small electron barrier between the lowest unoccupied molecular orbital (LUMO) of the $PC_{71}BM$ (4.2–4.3 eV) and the WF of the Al.[14,15] However, the use of Ag and Au cathodes yielded a low V_{oc} due to the unaligned energy levels between the LUMO of the $PC_{71}BM$ and the high WF of the cathodes. Such a mismatch can lead to inefficient charge transport due to non-ohmic contact at the organic semiconductor/high WF metal interface. Eventually, the PCEs dropped from 3.98% with the Al electrode to 2.77% and 1.72% for the Ag and Au electrodes, respectively.

Relative to the control devices, the introduction of a TiO_x symmetry breaking layer beneath the cathodes led to an increase in the J_{sc} from 9.72 to 10.5 mA cm^{-2} for Al, 9.32 to 10.1 mA cm^{-2} for Ag, and 9.2 to 9.5 mA cm^{-2} for Au. Similarly, the FF improved from 0.50 to 0.63 for Al, 0.45 to 0.55 for Ag, and 0.34 to 0.40 for Au. In addition, the V_{oc} ranged from 0.81 to 0.84 eV for the solar cells with Al, Ag, and Au cathodes and a TiO_x layer (Fig. 2b). The V_{oc} is thus independent of the cathode WF, while the J_{sc} and FF of the devices with TiO_x/Ag and TiO_x/Au are inferior to those of

the device with TiO_x/Al. It is likely that insufficient electrical contact is made with the Ag or Au cathode and thus, a high contact resistance exists at the interface between the LUMO of the $PC_{71}BM$ and the modified WF of the TiO_x/Ag and TiO_x/Au. Nonetheless, improvements in the PCEs of all devices incorporating a TiO_x layer were observed up to 5.56% for TiO_x/Al, 4.55% for TiO_x/Ag, and 3.15% for TiO_x/Au relative to those of the control devices (without an interlayer).

The dark J–V characteristics of the devices with and without an interlayer were also examined in order to gain further insight into the effects of the metal WFs modified by the interlayer (ESI†, Fig. S2). The dark currents with the TiO_x layer were significantly suppressed (<0.8 V region), implying a reduced leakage current. Such a positive effect can be attributed to the elimination of metal diffusion into the organic semiconductor layer from the cathode during thermal evaporation and a reduction in the probability of hole and electron recombination near the organic semiconducting/cathode interface.[16,17] Thus, the reduction in the dark current via the introduction of a proper interlayer near the metal electrodes may increase the V_{oc}. A similar increase in the V_{oc} has also been reported in polymer BHJ devices utilizing various interlayers (such as LiF), metal oxides, and conjugated polyelectrolytes.[11,18–21] One possible explanation for such an increase in the V_{oc} is the reduction in the WF of the metals due to the formation of interfacial dipoles between the organic semiconducting materials and the metal electrodes.

In order to explore the influence of an inserted TiO_x layer on energy level alignment, we performed ultraviolet photoelectron spectroscopy (UPS) measurements, which have been used to probe the interfacial properties induced by dipole formation.[22,23] The normalized UPS spectra for TiO_x/Al, TiO_x/Ag, and TiO_x/Au films, where Al, Ag, and Au were used as a reference, are shown in Fig. 3. The Fermi energy (E_F) was determined from the Au surface and all other spectra were plotted with respect to this value. The obtained WFs for Au, Ag, and Al were 4.90, 4.72, and 3.78 eV, which are different from the commonly cited values of 5.1, 4.6, and 4.2 eV, respectively.[24–26] It is well known that the WF of a metal can be changed by carbon and oxygen contamination at the surface.[27,28] After TiO_x deposition, the shifts in the vacuum levels (VLs) between the TiO_x and the metals changed significantly (the VL of the
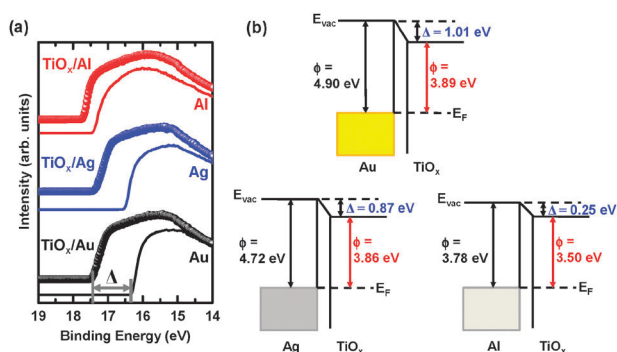

Fig. 3 (a) High binding energy region of the normalized UPS spectra of TiO_x/Al, TiO_x/Ag, and TiO_x/Au films; Al, Ag, and Au were used as references. (b) Schematic energy levels of TiO_x/Al, TiO_x/Ag, and TiO_x/Au films with an interfacial dipole (Δ); E_{vac}: vacuum level, E_F: Fermi level, ϕ = work function.

samples was determined by linear extrapolation of the secondary electron cutoffs on the high binding energy side (14–19 eV)). The shift in the VLs is indicative of the magnitude of the interfacial dipole (Δ).[22,23,27,28] The observed values of the interfacial dipole and modified WF are summarized in Fig. 3b. The strongest interfacial dipole was observed for the TiO_x/Au interface, while the TiO_x/Al interface exhibited the weakest dipole. Although the WF of TiO_x/Al (3.5 eV) was 0.3 eV smaller, the WFs of TiO_x/Au and TiO_x/Ag were almost constant (3.89 eV and 3.86 eV, respectively). It is thus suggested that a reduction in the WFs through the introduction of a TiO_x layer causes an increase in the V_{oc}.[29,30]

The solar cell parameters and results from dark current and UPS measurements are listed in Table 1. The shunt resistance (R_{sh}) and series resistance (R_s) were obtained from the inverse slope near 0 V and the V_{oc} in the dark current measurements, respectively. In Table 1, one can see that R_{sh} and R_s increased in the devices with a TiO_x layer. Since the R_s is related to the saturation current density and TiO_x is known to be a hole blocking material,[31,32] the reduction in current corresponds to inefficient hole accumulation and an increase in the R_s. In addition, the insertion of a TiO_x layer increased the R_{sh} due to the suppression of the leakage current, which is a requirement of a good solar cell. Therefore, the TiO_x induced an interfacial dipole at the organic semiconductor/metal interfaces that modified the effective WFs and improved the contact at the interface. Thus, devices with a larger V_{oc} and PCE were obtained.

The WF dependence of the V_{oc} and schematics of the energy levels for the devices in this work are shown in Fig. 4.

In the absence of an interfacial dipole, the V_{oc} scales linearly with the WF difference. It is generally believed that the V_{oc} is determined by the energy level difference between the highest occupied molecular orbital (HOMO) level of the donor and the LUMO level of the acceptor (see Fig. 4b).[33,34] However, our results indicate that the V_{oc} tends to be strongly correlated

Table 1 Summary of device performance and the electronic properties for each cathode without and with a TiO_x layer

	TiO_x/Al	Al	TiO_x/Ag	Ag	TiO_x/Au	Au
WF^a/eV	3.50	3.78	3.86	4.72	3.89	4.90
J_{sc}^b	10.5	9.72	10.1	9.32	9.5	9.2
V_{oc}/V	0.84	0.82	0.81	0.66	0.83	0.55
FF	0.63	0.50	0.55	0.45	0.40	0.34
PCE (%)	5.56	3.98	4.55	2.77	3.15	1.72
R_{sh}^c	0.12	0.02	0.06	0.07	2.5	0.10
R_s^d	71	92	77	74	4199	381

^{a} WF was determined by UPS analysis. ^{b} mA cm^{-2}. ^{c} MΩ cm^2. ^{d} Ω cm^2.
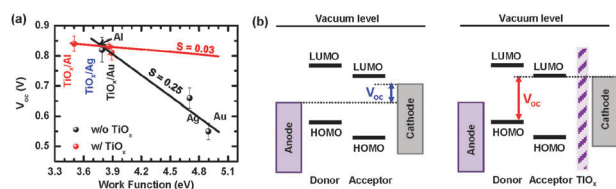

Fig. 4 (a) Plot of V_{oc} vs. cathode work functions. The solid lines were linearly fitted from the data. Error bars denote a standard deviation within 3%. (b) Schematic models of the V_{oc} in a donor/acceptor BHJ solar cell without and with a TiO_x interlayer.
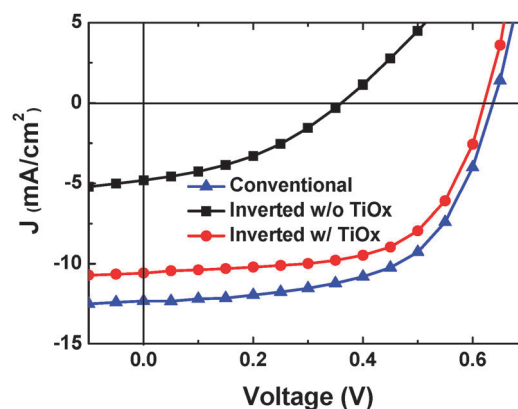

Fig. 5 J–V characteristics of the P3HT:PCBM inverted solar cells without and with the TiO_x interlayer under illumination. For comparison, the result obtained from the device with conventional structure is also included.

with the WF of the cathode. In Fig. 4a, the presence of an interfacial dipole due to the TiO_x leads to a slope that is almost zero. Such a result is attributed to a V_{oc} that is constant regardless of the cathode WF and is in agreement with the relationship $V_{oc} \approx$ HOMO (donor) – LUMO (acceptor). It is worth noting that the Fermi level of the TiO_x is pinned close to that of the LUMO of the $PC_{71}BM$ and the V_{oc} can be independent of any of the cathodes with a WF lower than the LUMO of $PC_{71}BM$.

The effect of a symmetry breaking layer is more critical in inverted solar cells. In order to confirm that the observed results are general, we have applied a TiO_x symmetry breaking layer on an inverted solar cell fabricated using other semi-conducting polymers poly(3-hexylthiophene) (P3HT) and [6,6]-phenyl-C_{61}-butyric methyl ester (PCBM). Fig. 5 shows the J–V characteristics obtained under illumination for inverted P3HT:PCBM solar cells that were fabricated with and without a TiO_x symmetry breaking layer (ITO/with or without TiO_x/P3HT:PCBM/PEDOT:PSS/Ag). The result obtained from the device with conventional structure of ITO/PEDOT:PSS/ P3HT:PCBM/TiO_x/Al is also included for comparison. For the inverted solar cell without the TiO_x layer, since we used Ag which has a similar WF to ITO as an electrode, no symmetry breaking was created, thereby showing significantly decreased photovoltaic parameters. However, a comparison of inverted solar cell characteristics between the devices with the TiO_x layer and without the TiO_x layer clearly indicates that the insertion of a TiO_x layer yields an increase in both J_{sc} and V_{oc} approaching those obtained from the solar cell with conventional structure. Therefore, we concluded that the inserted TiO_x layer led to symmetry breaking, thereby enhancing photovoltaic properties similar to the PCDTBT:$PC_{71}BM$ solar cells.

In summary, we demonstrated a correlation between the V_{oc} and the WF of the electrode by introducing a TiO_x symmetry breaking layer. The TiO_x leads to the formation of an interfacial dipole at the organic semiconductor/metal interfaces that modifies the effective WFs and improves device performance. Among the several photovoltaic parameters, the V_{oc} was most strongly influenced by symmetry breaking. However, with sufficient symmetry breaking, the influence of the cathode WF on the V_{oc} can be effectively reduced. Therefore, establishing sufficient

symmetry breaking is one of the most important factors for extracting a maximum V_{oc} and fabricating highly efficient BHJ solar cells, regardless of whether a conventional or inverted structure is utilized.

Notes and references

1 D. Gendron and M. Leclerc, *Energy Environ. Sci.*, 2011, **4**, 1225.
2 C. J. Brabec, S. Gowrisanker, J. J. M. Halls, D. Laird, S. Jia and S. P. Williams, *Adv. Mater.*, 2010, **22**, 3839.
3 A. C. Mayer, S. R. Scully, B. E. Hardin, M. W. Rowell and M. D. McGehee, *Mater. Today*, 2007, **10**, 28.
4 S. H. Park, A. Roy, S. Beaupré, S. Cho, N. Coates, J. S. Moon, D. Moses, M. Leclerc, K. Lee and A. J. Heeger, *Nat. Photonics*, 2010, **3**, 297.
5 J. Y. Kim, K. Lee, N. E. Coates, D. Moses, T.-Q. Nguyen, M. Dante and A. J. Heeger, *Science*, 2007, **317**, 222.
6 Y. Liang, Z. Xu, J. Xia, S.-T. Tsai, Y. Wu, G. Li, C. Ray and L. Yu, *Adv. Mater.*, 2010, **22**, E135.
7 H.-Y. Chen, J. Hou, S. Zhang, Y. Liang, G. Yang, Y. Yang, L. Yu, Y. Wu and G. Li, *Nat. Photonics*, 2009, **3**, 649.
8 N. S. Sariciftci, L. Smilowitz, A. J. Heeger and F. Wudl, *Science*, 1992, **258**, 1474.
9 L.-M. Chen, Z. Hong, G. Li and Y. Yang, *Adv. Mater.*, 2009, **21**, 1434.
10 Y. Sun, J. H. Seo, C. J. Takacs, J. Seifter and A. J. Heeger, *Adv. Mater.*, 2011, **23**, 1679.
11 H. Choi, J. S. Park, E. Jeong, G.-H. Kim, B. R. Lee, S. O. Kim, M. H. Song, H. Y. Woo and J. Y. Kim, *Adv. Mater.*, 2011, **23**, 2759.
12 (*a*) S. Cho, J. H. Seo, K. Lee and A. J. Heeger, *Adv. Funct. Mater.*, 2009, **19**, 1459; (*b*) S. Cho, K. Lee and A. J. Heeger, *Adv. Mater.*, 2009, **21**, 1941.
13 S. Cho, J. Yuen, J. Y. Kim, K. Lee, A. J. Heeger and S. Lee, *Appl. Phys. Lett.*, 2008, **92**, 063505.
14 M. O. Reese, M. S. White, G. Rumbles, D. S. Ginley and S. E. Shaheen, *Appl. Phys. Lett.*, 2008, **92**, 053307.
15 J. H. Seo, A. Gutacker, B. Walker, S. Cho, A. Garcia, R. Yang, T.-Q. Nguyen, A. J. Heeger and G. C. Bazan, *J. Am. Chem. Soc.*, 2009, **131**, 18220.
16 C. J. Brabec, S. E. Shaheen, C. Winder, N. S. Sariciftci and P. Denk, *Appl. Phys. Lett.*, 2002, **80**, 1288.
17 S.-H. Oh, S.-I. Na, J. Jo, B. Lim, D. Vak and D.-Y. Kim, *Adv. Funct. Mater.*, 2010, **20**, 1997.
18 X. Yang, J. Loos, S. C. Veenstra, W. J. H. Verhees, M. M. Wienk, J. M. Kroon, M. A. J. Michels and R. A. J. Janssen, *Nano Lett.*, 2005, **5**, 579.
19 C.-C. Chang, C.-F. Lin, J.-M. Chiou, T.-H. Ho, Y. Tai, J.-H. Lee, Y.-F. Chen, J.-K. Wang, L.-C. Chen and K.-H. Chen, *Appl. Phys. Lett.*, 2010, **96**, 263506.
20 M. S. White, D. C. Olson, S. E. Shaheen, N. Kopidakis and D. S. Ginley, *Appl. Phys. Lett.*, 2006, **89**, 143517.
21 J. H. Seo, A. Gutacker, Y. Sun, H. Wu, F. Huang, Y. Cao, U. Scherf, A. J. Heeger and G. C. Bazan, *J. Am. Chem. Soc.*, 2011, **133**, 8416.
22 J. H. Seo and T.-Q. Nguyen, *J. Am. Chem. Soc.*, 2008, **130**, 10042.
23 H. Ishii, K. Sugiyama, E. Ito and K. Seki, *Adv. Mater.*, 1999, **11**, 605.
24 J. Hwang, A. Wan and A. Kahn, *Mater. Sci. Eng., R*, 2009, **64**, 1.
25 J. Huang, Z. Xu and Y. Yang, *Adv. Funct. Mater.*, 2007, **17**, 1966.
26 K. Sugiyama, H. Ishii, Y. Ouchi and K. Seki, *J. Appl. Phys.*, 2000, **87**, 295.
27 J. H. Seo, R. Yang, J. Z. Brzezinski, B. Walker, G. C. Bazan and T.-Q. Nguyen, *Adv. Mater.*, 2009, **21**, 1006.
28 W. R. Salaneck, M. Lögdlund, M. Fahlman, G. Greczynski and Th. Kugler, *Mater. Sci. Eng., R*, 2001, **34**, 121.
29 C. Tengstedt, W. Osikowicz, W. R. Salaneck, I. D. Parker, C.-H. Hsu and M. Fahlman, *Appl. Phys. Lett.*, 2006, **88**, 053502.
30 S. Toyoshima, K. Kuwabara, T. Sakurai, T. Taima, K. Saito, H. Kato and K. Akimoto, *J. Jpn. Appl. Phys.*, 2007, **46**, 2692.
31 J. H. Lee, S. Cho, A. Roy, H.-T. Jung and A. J. Heeger, *Appl. Phys. Lett.*, 2010, **96**, 163303.
32 C. He, C. Zhong, H. Wu, R. Yang, W. Yang, F. Huang, G. C. Bazan and Y. Cao, *J. Mater. Chem.*, 2010, **20**, 2617.
33 M. C. Scharber, D. Mühlbacher, M. Koppe, P. Denk, C. Waldauf, A. J. Heeger and C. J. Brabec, *Adv. Mater.*, 2008, **18**, 789.
34 S. R. Cowan, A. Roy and A. J. Heeger, *Phys. Rev. B: Condens. Matter*, 2010, **82**, 245207.